Novel Colloidal Materials from Functionalized Polyoxometalates

LaSalle Swenson,[a] Jose Orozco,[a] Yuzi Liu,[b] Seth B. Darling[b,c] and M. Ishaque Khan*[,a]

[a]Department of Chemistry, Illinois Institute of Technology, Chicago, IL, 60616, USA
[b]Center for Nanoscale Materials, Argonne National Laboratory, Argonne, IL, 60439, USA
[c]Institute for Molecular Engineering, The University of Chicago, Chicago, IL, 60637, USA

† Supplementary information (SI) available: complete synthetic details for **1** and **2**. TGA, FTIR and Transmission and reflectance UV-vis analyses.

Novel colloidal materials were prepared for the first time from the organo-functionalized Anderson structure polyoxometalate species $[NaV^{IV}_6O_6\{(OCH_2CH_2)_2N(CH_2CH_2OH)\}_6]Cl{\bullet}H_2O$ and the mixed-addenda Keggin structure polyoxometalate, $K_4(PVW_{11}O_{40})$. The materials were characterized by SEM, TGA, FTIR and UV-vis spectroscopy. The colloidal materials are readily separated from suspension in the form of redistributable micrometer-scale monoliths, which may be considered a type of POM heterogenation. The monoliths are insoluble in low polarity media and lower aliphatic alcohols and readily form thin-films ($\delta < 100$ um) by solvent casting.

Polyoxometalates (POM) are transition metal-oxide clusters, formed mainly by the early transition metals V, Mo, and W, usually in their highest (d^0) oxidation state.[1, 2] POMs are large molecular systems of dimensions up to several nanometers and which exhibit extensive electrochemistry, rich electronic spectroscopy, and diverse structural types. POM contain redox centers,[1, 2] absorb in the near-UV,[1, 2] and have applications in a variety of technical areas, including catalysis,[3, 4] photocatalysis,[5] biomedicine,[6] and magnetism.[7] As discreet molecular units having well-defined chemical properties, POMs are attractive building blocks for new materials whose properties could possibly be rationalized in terms of their constituents at the molecular level.[6, 8, 9] For example, POMs have appeared as both framework constituents and encapsulated species in framework materials (*viz.* metal-POM,[8, 10-14] POM-organic,[8] metal-organic,[9, 15] and covalent organic[16] framework materials). In the colloidal realm, organo-derivatized and surfactant-encapsulated POM have been shown to self-assemble diverse

nanostructures in various solvent systems through solvo-phobic(philic) interactions;[17-19] larger POMs—so called POM macroions—self-assemble vesicle-like nanostructures through counter ion-mediated attraction.[18, 20] These prior colloid examples are fragile in nature, relying on solvent interactions to maintain their form. Here we report the self-assembly of (sub)micrometer scale colloidal materials from POM species in the form of isolable and redistributable monoliths. The new materials are readily synthesized and isolated in sub-gram quantities. Strong interparticle attraction makes the colloids inherently thin film-forming upon drying of colloidal suspensions.

We have reported a series of organo-functionalized polyoxovanadium(IV) compounds, which included $[NaV^{IV}_6O_6\{(OCH_2CH_2)_2N(CH_2CH_2OH)\}_6]Cl{\bullet}H_2O$ (**NaV_6**).[21] **NaV_6** contains a fully reduced cyclic $\{NaV_6N_6O_{18}\}$ framework comprised of a ring of six edge-sharing $\{V^{IV}O_5N\}$ octahedra encapsulating a Na^+ ion forming an Anderson-like structure (Fig. 1a). The oxovanadium framework in **NaV_6** covalently incorporates six triethanolamine ligands forming the cationic cluster, $[NaV^{IV}_6O_6\{(OCH_2CH_2)_2N(CH_2CH_2OH)\}_6]^+$. The two $\{O\text{-}CH_2\text{-}CH_2\text{-}\}$ arms of each of the triethanolamine ligands decorate the metallocyclic ring $\{NaV_6O_6\}$, the third $\{HO\text{-}CH_2\text{-}CH_2\text{-}\}$ arm remains pendant. **NaV_6** absorbs in the visible and near-UV[22] and shows ferromagnetic behavior below room temperature.[21] In view of the interesting structural, electronic, and magnetic properties of these organo-functionalized polyoxovanadium(IV) compounds, we are investigating their potential as building units for new functional materials. During the course of this work, we discovered two new polyoxometalate based colloidal materials, described here. The first of these two materials (**1**), derived from **NaV_6**, contains intact units of the polyoxocation $[NaV^{IV}_6O_6\{(OCH_2CH_2)_2N(CH_2CH_2OH)\}_6]^+$. The second material (**2**), obtained by combining **NaV_6** with the Keggin structure (Fig. 1b) species $K_4(PVW_{11}O_{40})$ (**VW_{11}**)[23], is a composite of the polyoxocation, $[NaV^{IV}_6O_6\{(OCH_2CH_2)_2N(CH_2CH_2OH)\}_6]^+$, and the polyoxoanion, $PVW_{11}O_{40}^{4-}$.

The colloidal material **1** was prepared by a benchtop procedure by lowering the pH of an aqueous solution of $[NaV^{IV}_6O_6\{(OCH_2CH_2)_2N(CH_2CH_2OH)\}_6]Cl{\bullet}H_2O$ (NaV_6) (see **SI** for synthetic details). The initially clear blue solution of NaV_6 assumed a slightly aquamarine color as the pH was lowered, followed by a sudden clouding, indicating precipitate formation. The lime-green, gelatinous precipitate was readily isolated by low-speed (< 3000 RPM) centrifugation (see

Scheme 1, steps a-d). Upon drying, the precipitate formed a gel of uniform appearance (Fig. 1c), which finally assumed the form of a semi-continuous layer (Fig. 1d). The material spontaneously separates from the polystyrene petri dish and tends to curl in on itself. The two-dimensional, self-supporting form shows that **1** is inherently thin-film forming upon drying. The material is readily redistributed in water (see Scheme 1, steps e-f) and is indefinitely stable at low pH. Thicker layers, having greater in-plane continuity, may be obtained by drying redistributed material. The curled layers can withstand a degree of forced coiling and uncoiling without breaking, and indicate elasticity. Layer flexibility and elasticity is demonstrated by its repeated (partial) coiling and uncoiling by force of electrostatic attraction (Fig. 1g). In cylindrical coordinates, this motion indicates flexibility and elasticity along the r and θ directions. The coiled piece of Figure 1g (mass = 32 mg) has a superficial length of around 4 cm and is less than 40 μm thick (SEM), giving it an aspect ratio greater than 1000.

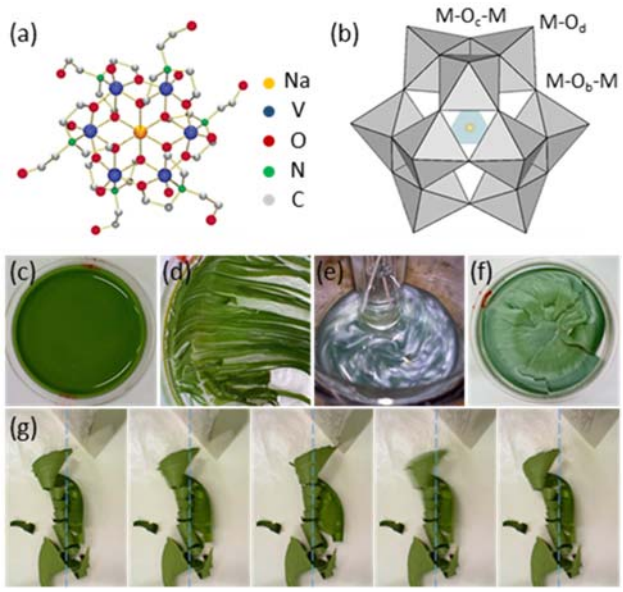

Fig. 1. (a) Ball-and-stick view of the polyoxocationic core $[NaV^{IV}_6O_6\{(OCH_2CH_2)_2N(CH_2CH_2OH)\}_6]^+$ of $[NaV^{IV}_6O_6\{(OCH_2CH_2)_2N(CH_2CH_2OH)\}_6]Cl{\bullet}H_2O$ (**NaV_6**). (b) Polyhedral representation of a Keggin structure polyoxoanion. The Keggin anion contains four 3-fold M_3O_{13} groups linked by corner-sharing (the fourth M_3O_{13} group is not shown

for clarity). The four identifying vibrational bands are associated with: the central tetrahedron (XO_4); the three terminal oxygen atoms of each M_3O_{13} group (M-O_d); the peripheral bridging bonds between edge-sharing oxygen atoms (M-O_c-M); and the bridging bonds between corner-sharing octahedra (M-O_b-M). Optical images of **1** and **2** (c-g). Acidification of a solution of **NaV_6** (clear, blue) results in a green gelatinous precipitate of uniform appearance (c). Ambient drying of the gel results in high aspect ratio structures. In (d) the dried layer has separated into pieces having the geometry of a thin flat blade of grass and which detach unassisted from the polystyrene petri dish (47 mm I.D.). The pieces display flexibility and elasticity along the non-planar dimension (i.e., the short dimension perpendicular to the plane of the dish). (e) Colloid formation is indicated by strong opalescence under stirring during the synthesis of **2**, derived from a mixture of $[NaV^{IV}_6O_6\{(OCH_2CH_2)_2N(CH_2CH_2OH)\}_6]Cl{\bullet}H_2O$ (**NaV_6**) and $K_4(PW_{11}VO_{40})$ (**V_1W_{11}**) (yellow). (f) The dried material **2** forms a semi-continuous layer that separates readily from the petri dish. Video stills sequence showing the coiling and uncoiling of **1** under the force of electrostatic attraction (g). The full video is available as Supplementary Material.

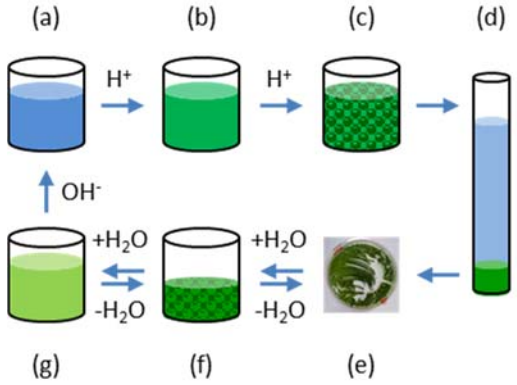

Scheme 1. Reversible synthesis of colloid **1** from the functionalized cluster $[NaV^{IV}_6O_6\{(OCH_2CH_2)_2N(CH_2CH_2OH)\}_6]Cl{\bullet}H_2O$ (**NaV_6**).

SEM micrographs of the coiled piece shown in Fig. 1g show that it is composed of discreet, irregular planar monoliths with planar dimensions generally less than 10 μm and thicknesses of around 1 μm (Fig. 2a-b). No apparent order of monolith arrangement is indicated in either the

planar (Fig. 2a) or profile (Fig. 2b) views of **1**. The extended structure and flexibility of **1**, and its insolubility in weakly polar media imply attractive surface interactions between contacting monoliths. FTIR-ATR spectra of **NaV_6** and **1** show that **1** contains the intact polyoxocation cluster, $[NaV^{IV}_6O_6\{(OCH_2CH_2)_2N(CH_2CH_2OH)\}_6]^+$ (Fig. 3a-b). Given the six pendant ethanolic arms of each cluster, we anticipate a monolith surface rich in polar alcohol groups capable of supporting hydrogen bonds. Around three molecules of water are present per polyoxocation cluster (TGA, see SI). The soft-chemical nature of the synthesis of **1** suggests an entropic driving force. In this regard, we observe that the $[NaV^{IV}_6O_6\{(OCH_2CH_2)_2N(CH_2CH_2OH)\}_6]^+$ polyoxocation contains both hydrophilic (metal oxide core, hydroxyl groups) and hydrophobic (18{-CH2-CH2-} hydrocarbon moities) regions. The FTIR (ATR and transmission) spectrum of **1** contains a distinguishing band centered near 830 cm^{-1} that is absent from the spectrum of **NaV_6**. Transmission mode FTIR (KBr method) spectra indicate that the magnitude of the 830 cm^{-1} band of **1** decreases disproportionately upon annealing (Fig. S7). The origin of this band and the decrease in its intensity upon annealing is under further investigation and the results will be presented in a future paper. SEM micrographs of samples of **1** drawn directly form suspension show colloidal monoliths of the same general shape and size indicated in Fig. 1a and b—irregular planar monoliths with planar dimensions generally less than 10 μm and thicknesses of around 1 μm (Fig. 2e). TEM micrographs of **1** drawn from highly dilute (5×10^{-5} M) suspensions at low pH indicated the tendency of **NaV_6** clusters to aggregate, consistent with the observed formation of colloids upon pH reduction (Fig. S8).

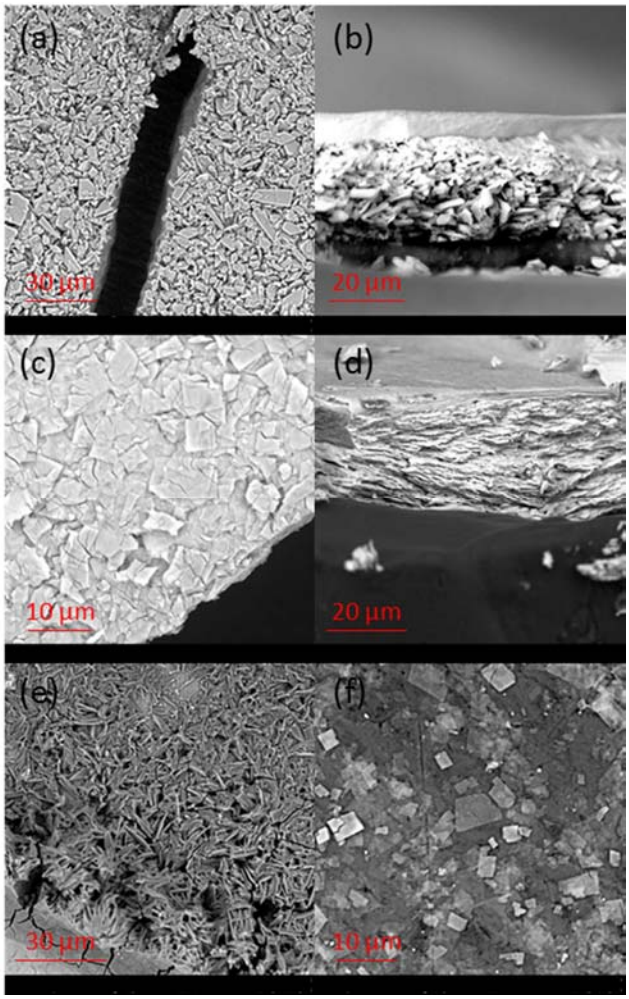

Fig. 2. SEM micrographs of **1** (a-c) and **2** (d-f)). Planar (a) and profile (b) views of the semicontinuos layer formed by **1**. Planar (d) and profile (e) views of the semi-continuous layer formed by **2**. Dilute dispersions of **1** (c) and **2** (f) dropped directly onto the surface of the SEM sample holder and dried under ambient conditions.

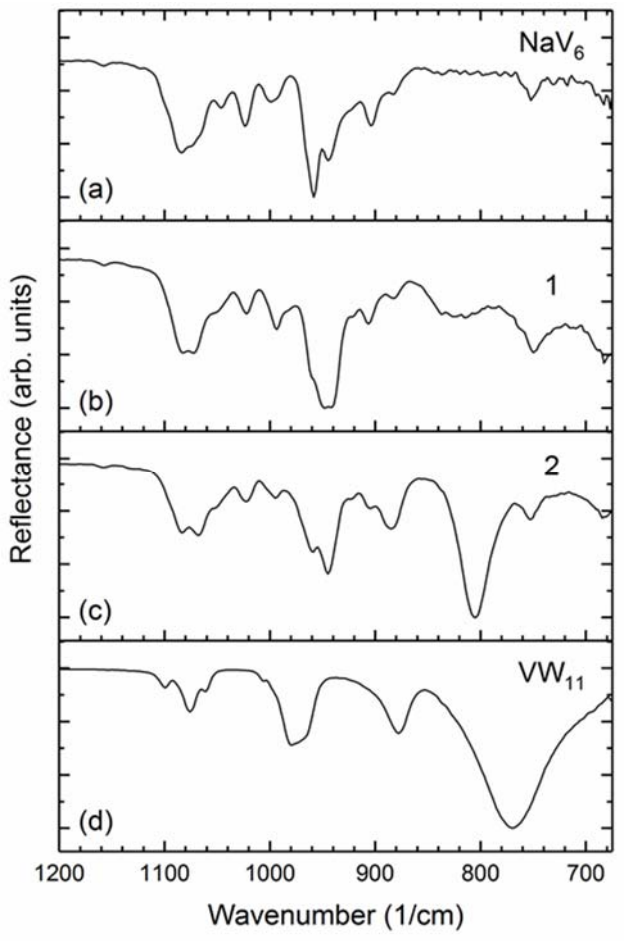

Fig. 3. FTIR-ATR spectra of **NaV_6** (a), **1** (b), **2** (c), and **VW_{11}** (d) in the 1200 - 675 cm^{-1} range.

Dilution of a suspension of **1** with neutral water (pH ~ 6.2) to about 0.5 mg/ml reverses colloid formation and produces a clear lime green liquid phase (hereafter **1G**) having the appearance of a solution (Scheme 1, f-g). The blue to aquamarine color change of the **NaV_6** solution upon lowering pH during the synthesis of **1**, identifies **1G** as an intermediate in the formation of the colloidal material **1**. The aqueous transmission spectra of **1G** and **NaV_6** both contain the 610 nm band that is characteristic of **NaV_6** and originates in d-d transitions at the reduced vanadium (V^{IV}) addenda (Fig. S9). Visible absorption, initiating around 525 nm, and overlapping the charge-transfer band is also observed in the **1G** spectrum (Fig. S9), consistent with its green colour. The aqueous phase transmission spectrum of **NaV_6** indicates a similar feature upon lowering pH;[22] we therefore attribute this absorption change to protonation of the

metallocyclic ring {NaV_6O_6} of **NaV_6** upon pH reduction during the synthesis of **1**, and identify the protonated form (**1G**) as a synthetic intermediate. We increased the pH of the **1G** solution by addition of aqueous NaOH and observed a color change from light green to light blue (Scheme 1, g-a), further confirming that protonation of **NaV_6** precedes colloid formation. We isolated a blue solid by evaporative crystallization and found that its FTIR spectrum was identical to that of **NaV_6** (Fig. S10). Thus the formation of **1** from **NaV_6** is reversible. Additionally, we transformed a **1G** solution to **1** by evaporative re-concentration (Scheme 1, g-e), further demonstrating the reversibility of the **NaV_6-1G-1** system.

The colloidal material **2** was made by mixing an aqueous solution of **NaV_6** with a yellow aqueous solution of **VW_{11}** in a ratio of 7:1 (see SI for synthetic details). Colloids formed within minutes of mixing the two solutions, as indicated by opalescence (Fig. 1e). The colloids were separated and refined by centrifugation. Like the colloidal material **1**, the dried product formed a semi-continuous solid layer (Fig. 1f). SEM micrographs show that **2** is composed of discreet, rectangular-planar, sheet-like monoliths with planar dimensions generally less than 5 μm and thicknesses of around 100 nm (Fig. 2c-d). Like **1**, the two-dimensional, self-supporting form shows that **2** is inherently thin-film forming upon drying. In contrast to the random orientations observed in **1**, the thinner monoliths of **2** have settled with their planar surfaces parallel (Fig. 2d). SEM micrographs of samples of **2** drawn directly form suspension show colloidal monoliths of the general shape and size as indicated in the micrographs of the semi-continuous layer (Fig. 2f). The FTIR-ATR spectrum of **2** shows contributions from both **NaV_6** and **VW_{11}** (Fig. 3). The feature peaking at 794 cm^{-1} in the **VW_{11}** spectrum appears blue-shifted (811 cm^{-1}) in the spectrum of **2**. This band is associated with bridging bonds between edge sharing octahedra (W-O_c-W). The M-O_d, M-O_b-M and M-O_c-M band locations of the Keggin structure (Figure 1b) are sensitive to Coulombic interactions;[24] it is thus common to observe band shifts when varying the chemical environment of the polyoxoanion.[25-30] Thus the FTIR spectral analysis indicates that material **2** is a composite composed of $[NaV^{IV}_6O_6\{(OCH_2CH_2)_2N(CH_2CH_2OH)\}_6]^+$ and $PW_{11}VO_{40}^{4-}$ constituents. Elemental analysis (XRF) indicates that the constituents are present in the ratio of 3.9:1 ($[NaV^{IV}_6O_6\{(OCH_2CH_2)_2N(CH_2CH_2OH)\}_6]^+$:$PW_{11}VO_{40}^{4-}$), consistent with the charge balance requirement of each constituent. **2** has no potassium present and a negligible amount of chlorine. The analytical and spectroscopic data agrees with a chemical

formula of $[NaV^{IV}_6O_6\{(OCH_2CH_2)_2N(CH_2CH_2OH)\}_6]_4(PW_{11}VO_{40})\cdot 16H_2O$ for **2**. The soft-chemical nature of the reaction forming **2** and the formula are consistent with a self-assembly process driven by intercluster electrostatic interactions.

A UV-vis reflectance spectral comparison of **NaV_6** and **1** is consistent with the presence of the intact $[NaV^{IV}_6O_6\{(OCH_2CH_2)_2N(CH_2CH_2OH)\}_6]^+$ cluster in **1** and the color of each species. The electronic spectra of **NaV_6**, **V_1W_{11}**, and **2** are consistent with the composite nature and color of **2**. There is no spectral evidence for any changes in the oxidation state of either **NaV_6** or **V_1W_{11}** upon forming **1** and **2**, consistent with the soft-chemical nature of the respective syntheses (see SI for complete discussion of the UV-vis reflectance spectra and Figure S11).

In summary, we have obtained colloidal materials directly from POM species by a soft-chemical, benchtop method. Colloidal material **1** is derived directly from the organo-functionalized Anderson structure polyoxometalate species $[NaV^{IV}_6O_6\{(OCH_2CH_2)_2N(CH_2CH_2OH)\}_6]Cl\bullet H_2O$. Colloidal material **2** is a composite derived from $[NaV^{IV}_6O_6\{(OCH_2CH_2)_2N(CH_2CH_2OH)\}_6]Cl\bullet H_2O$ and the mixed-addenda Keggin structure, $K_4(PVW_{11}O_{40})$. The colloids are in the form of micrometer-scale, (semi-)rectangular monoliths. Strong inter-monolith attractive forces are indicated by the self-assembly of high-aspect ratio structures upon dehydration of colloidal suspensions.

References

[1] M.T. Pope, Heteropoly and Isopoly Oxometalates, Springer Verlag, Berlin, 1983.

[2] Special thematic issue on polyoxometalates. C.L. Hill (Guest ed.), Chem. Rev. 98 (1998) 1-390.

[3] I.V. Kozhevnikov, Catalysis by Polyoxometalates, Catalysts for Fine Chemical Synthesis 2, John Wiley & Sons, West Sussex, England, 2002.

[4] J. B. Moffat, Metal-Oxygen Clusters: The Surface and Catalytic Properties of Heteropoly Oxometalates, Kluwer Academic Publishers, New York, 2001.

[5] G. Marci, E.I. Garcia-Lopez, L. Palmisano, Eur. J. Inorg. Chem. 2014 (2014) 21.

[6] N. Casan-Pastor, P. Gomez-Romero, Front. Biosci. 9 (2004) 1759.

[7] J.M. Clemente-Juan, E. Coronado, A. Gaita-Arino, Chem. Soc. Rev. 41 (2012) 7464.

[8] H.N. Miras, L. Vila-Nadal, L. Cronin, Chem. Soc. Rev. 43 (2014) 5679.

[9] D.Y. Du, J.S. Qin, S.L. Li, Z.M. Su, Y.Q. Lan, Chem. Soc. Rev. 43 (2014) 4615.

[10] Y. Wang, L. Ye, T.G. Wang, X.B. Cui, S.Y. Shi, G.W. Wang, J.Q. Xu, Dalton Trans. 39 (2010) 1916.

[11] Z. Zhang, M. Sadakane, T. Murayama, S. Izumi, N. Yasuda, N. Sakaguchi, W. Ueda, 53 (2013) 903.

[12] M.I. Khan, E. Yohannes, D. Powell, Chem. Commun. (1999) 23.

[13] M.I. Khan, E. Yohannes, R.J. Doedens, Angew. Chem. Int. Ed. 38 (1999) 1292.

[14] M.I. Khan, J. Solid State Chem. 152 (2000) 105.

[15] G. Férey, C. Mellot-Draznieks, C. Serre, F. Millange, J. Dutour, S. Surblé, I. Margiolaki, 309 (2005) 2040.

[16] H. Ma, B. Liu, B. Li, L. Zhang, Y.-G. Li, H.-Q. Tan, H.-Y. Zang, G. Zhu, J. Am. Chem. Soc. 138 (2016) 5897.

[17] P.C. Yin, A. Bayaguud, P. Cheng, F. Haso, L. Hu, J. Wang, D. Vezenov, R.E. Winans, J. Hao, T. Li, Y.G. Wei, T.B. Liu, Chem. Eur. J. 20 (2014) 9589.

[18] P. Yin, D. Li, T. Liu, Chem. Soc. Rev. 41 (2012) 7368.

[19] Y. Yan, L. Wu, Israel J. Chem. 51 (2011) 181.

[20] Z.N. Liu, T.B. Liu, M. Tsige, Sci. Rep. 6 (2016).

[21] M.I. Khan, S. Tabussum, R.J. Doedens, V.O. Golub, C.J. O'Connor, Inorg. Chem. 43 (2004) 5850.

[22] L. Swenson, J.C. Orozco, J.A. Kaduk, M.I. Khan, Inorg. Chim. Acta. 444 (2016) 43.

[23] $K_4(PVW_{11}O_{40})$ (VW_{11}) contains the Keggin structure heteropoly anion $PVW_{11}O_{40}^{4-}$. $PVW_{11}O_{40}^{4-}$ undergoes reversible one-electron reduction at 0.58 V (vs. SCE) to form $PV^{IV}W_{11}O_{40}^{5-}$ (D.P. Smith, M. T. Pope, Inorg. Chem. 12 (1973) 331.) and has been investigated as a photo-catalyst (M. Schulz, C. Paulik, G. Knor, J. Mol. Catal. A: Chem. 347 (2011) 60.

[24] C. Rocchiccioli-Deltcheff, M. Fournier, R. Franck, R. Thouvenot, Inorg. Chem. 22 (1983) 207.

[25] M. Hasik, A. Pron, J. Pozniczek, A. Bielanski, Z. Piwowarska, K. Kruczala, R. Dziembaj, J. Chem. Soc. Faraday Trans. 90 (1994) 2099.

[26] M. Clemente-León, B. Agricole, C. Mingotaud, C.J. Gómez-García, E. Coronado, P. Delhaes, Langmuir 13 (1997) 2340.

[27] W. Feng, T. Zhang, Y. Liu, R. Lu, C. Guan, Y. Zhao, J. Yao, Mater. Chem. Phys. 77 (2003) 294.

[28] Y. Wang, C. Guo, Y. Chen, C. Hu, W. Yu, J. Colloid Interface Sci. 264 (2003) 176.

[29] T. Akutagawa, D. Endo, H. Imai, S.-i. Noro, L. Cronin, T. Nakamura, Inorg. Chem. 45 (2006) 8628.

[30] Y. Zhao, W. Qi, W. Li, L. Wu, Langmuir, 26 (2010) 4437.